1st Civil and Environmental Engineering Student Conference
25-26 June 2012
Imperial College London

Factors controlling the occurrence of reservoir-induced seismicity

X. Qiu

ABSTRACT

Reservoir-induced seismicity (RIS) is triggered by a complex interaction between a number of diverse factors: reservoir size, stress regime, hydrogeological condition and reservoir-filling history. This paper focuses on the relationship between these factors and the occurrence of RIS, based on the statistical evaluation of worldwide data and a detailed case analysis of the Xinfengjiang reservoir in China. There is a strong correlation between the occurrence of RIS and inducing factors such as reservoir size, faulting regimes and rock types. However these factors alone are certainly not necessary nor sufficient conditions for the triggering of RIS. As the interactions between water movement and geology can be significantly complex, a detailed study on the Xinfengjiang reservoir is presented as an illustrative case history. Examination of fault location, orientation and permeability structure indicate that the NNW Shijiao-Xingang-Baitian fault is responsible for the majority of seismic events, including the M_S 6.1 main shock on 19th March 1962. This result indicates the importance of hydrogeological conditions in triggering seismicity.

The fracture permeability in the reservoir region is estimated to range from 5×10^{-15} m^2 to 2.5×10^{-14} m^2 which is within the seismogenic permeability range suggested by Talwani et al. (2007). By constructing a simple Mohr-Coulomb failure model, it can be seen the vertical elastic stress increase caused by the reservoir impoundment will not trigger RIS in the Xinfengjiang area which is classified as a strike-slip faulting regime. By comparing the magnitudes of undrained pore pressure increase and the diffused pore pressure increase, the dominant mechanism for inducing the M_S 6.1 main shock is identified to be time-dependent pore pressure diffusion. By modelling the pore pressure diffusion history, it is found that prior to the occurrence of the M_S 6.1 main shock, although reservoir water level was decreasing, the diffused pore pressure at the hypocentre was still increasing. The evolution of the hydrogeological regime beneath reservoirs experiencing RIS is complex and often site-specific. In order to accurately assess the risk of RIS, it might not be sufficient to consider a single factor, such as hydrogeological conditions. It is therefore advised that all concurring factors should be taken into account for a reliable and comprehensive assessment.

1. INTRODUCTION

Reservoir-induced seismicity (RIS) is defined as the failure of a pre-existing fault due to the presence of a reservoir impoundment or water level fluctuations. Up to now, there have been 127 RIS cases reported around the world. Among them, 4 cases of strong earthquakes (M≥6), 15 cases of moderate earthquakes (5.9≥M≥5) and 32 cases of light earthquakes (4.9≥M≥4) can be found (Qiu, 2012).

The main aim of this paper is to assess whether there exists any specific tectonic settings, hydrogeological conditions or reservoir filling histories which are required for RIS to occur. Through the examinations of the observations recorded at different RIS sites around the world as well as the detail case study on Xinfengjiang reservoir, correlation between the occurrence of RIS and different inducing factors is assessed.

Investigation of the inducing factors of RIS can enhance our understanding of the mechanics of natural earthquakes, as well as the hydraulic properties of the crust. The advancements in the understanding of RIS can assist engineers in effectively mitigating the hazards of reservoir induced earthquakes through safe reservoir site selection and careful control of water level.

2. WORLDWIDE PATTERNS

2.1 Reservoir Size

RIS has occurred in reservoirs with varying dam heights. However the likelihood of RIS occurrence increases with increasing dam height. For shallow reservoirs with dam height less than 50m, the probability of RIS occurrence is the lowest. Only 0.05% of these reservoirs have reported RIS. On the other hand, 17% of the deep reservoirs with dam heights over 150m have triggered seismicity (Table 1). This trend shows that there is a positive correlation between dam height and probability of RIS occurrence.

Dam height (m)	Number of reservoirs	Number of RIS cases	Likelihood of RIS
≤50	33083	15	0.05%
50~100	3537	33	0.93%
100~150	573	37	6.46%
>150	187	32	17.11%

Table 1: Dam height and likelihood of RIS

A similar pattern is observed for reservoir capacity. Although there is a positive correlation between reservoir size (dam height & capacity) and probability of RIS occurrence, reservoir size is neither a necessary nor a sufficient condition for RIS to occur since many RIS cases is occurring in small-size reservoirs (capacity $\leqslant$1km^3) and many large-size reservoirs (capacity $\geqslant$10 km^3) do not trigger seismicity.

2.2 Faulting Regimes

Among the 127 RIS reservoir sites evaluated, 79% of the RIS reservoirs are located in normal or strike-slip faulting environments, while only 21% are in reverse faulting environments (Figure 1).

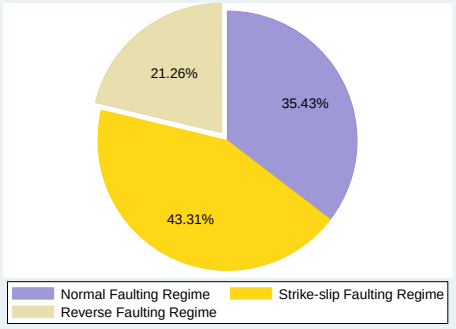

Figure 1: Tectonic setting (types of faulting) for 127 worldwide RIS cases

The phenomenon that reservoirs located in reverse faulting regimes are less susceptible to RIS than reservoirs in normal or strike-slip faulting regimes can be explained by constructing a simple Mohr-Coulomb failure model. In an environment of reverse faulting, the minimum principal stress is in the vertical direction. Reservoir impoundment will directly increase the minimum principal stress, thus decreasing the diameter of Mohr circle, moving it further away from the failure envelope (Figure 2). If pore pressure changes are small, reservoir impoundment may even stabilise the reservoir area. However RIS can still occur if pore pressure changes are significant or if the region is already very close to failure before reservoir impoundment.

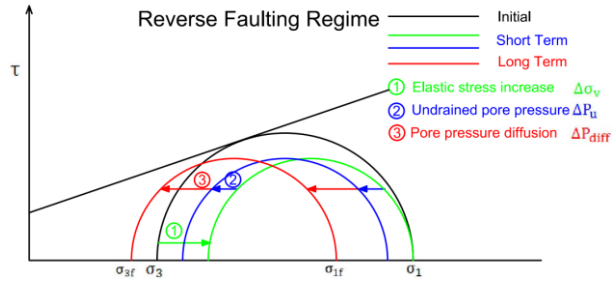

Figure 2: Evolution of stress field (assuming Mohr-Coulomb failure criteria) from reservoir impoundment in a reverse faulting regime

2.3 Rock Types

From the compiled global data set of 115 RIS cases, reservoir areas underlain by carbonate or crystalline rocks are most likely to experience RIS (Figure 3). Carbonate rocks are the most vulnerable rock type to chemical dissolution, which reduces cohesion and coefficient of friction, thus weakening the fault strength (Fyfe et al., 1978). The dissolved material may also be washed away by the undrained water flow, resulting in the widening of fractures, weakening of rock strength and increase in fracture permeability.

Most crystalline rocks, especially granite, cannot be treated as an equivalent porous medium as. In a large granite body, more than 80% of the water flow is contained in several major pre-existing fractures (Cornet & Yin, 1995). This significant amount of water flow makes the fractures in granite saturated and hence, often critically stressed and on the threshold of failure.

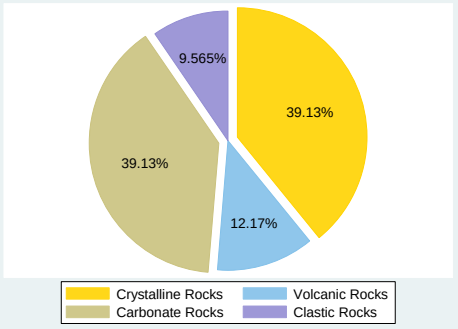

Figure 3: Rock types in reservoir regions experiencing RIS (115 cases worldwide)

3. XINFENGJIANG RESERVOIR, CHINA

Located in the southeast of China, Xinfengjiang reservoir has a capacity of 1.4×10^{10} m^3 and a dam height of 105 m. It is situated above a huge E-W trending Late Mesozoic age granite body. Soon after the impoundment in October 1959, an increase in earthquakes frequency in the region was observed. An earthquake of M_s 6.1 occurred on 19 March 1962, five months after the first peak water level. The main shock was on a steep, left lateral strike-slip fault striking NNW. The seismic activity level started to decrease after 1965 (Ding, 1989).

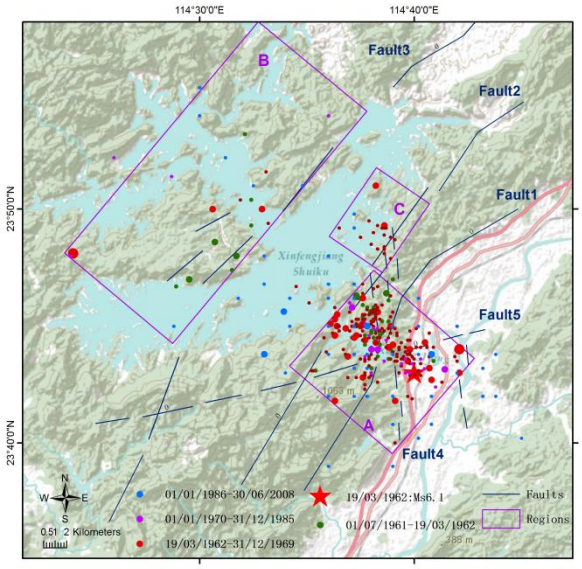

Figure 4: Distribution of epicentres of Ms≥3 earthquakes (Jul 1961 to Jun 2008) The numbered fault number are referred to in the following text)

3.1 Fault Features and Locations

Most of the earthquakes with M_s≥3 are located within three regions: A, B and C (Figure 4). These regions are closely associated with faults striking in three different directions. Region A is characterised by the intersection of three faults: the NE striking Heyuan fault (1), the ENE striking Nanshan-Aotou fault (5) and the NNW striking Shijiao-Xingang-

Baitian fault (4). Region B contains the NNE/NE striking Daping-Yanqian fault (3) and region C is associated with the NE striking Renzishi fault (2).

The features of major faults in the reservoir area are summarised from Ding (1989). The location of the fault relative to the reservoir determines whether the oscillating reservoir loads have a stabilising or destabilising effect (seismicity) on the fault (Roeloffs, 1988). In the case of normal faults and vertical strike-slip faults located below the reservoir, seismicity might be induced by the oscillating reservoir loads. However, if such faults are located at the reservoir edge, oscillating reservoir loads will stabilise the fault instead. In the case of a steeply dipping reverse fault, if the reservoir is located on its foot wall, then seismicity can be triggered. If the reservoir is located on the hanging wall, oscillating loads will exert a stabilising effect on the fault. In the case of a shallowly-dipping thrust fault, oscillating reservoir load-induced seismicity may require the reservoir to be situated on the hanging wall, otherwise the fault will be stabilised.

The Heyuan fault (1) is a shallowly-dipping (35° to 50°) thrust fault. The fault dips towards the SE with the reservoir located on its footwall. As a result, the oscillating reservoir load should not induce seismicity on the fault. Figure 4 shows that very few earthquakes occurred along Heyuan fault, except for the middle segment where the fault is intersected by Shijiao-Xingang-Baitian fault (4). This small segment is subjected to left lateral movement under the influence of Shijiao-Xingang-Baitian fault (4).

The Renzishi fault (2) is a steeply-dipping (60° to 80°) reverse fault. The northern segment of the fault is dipping towards SE, while the southern segment in the clastic formations is dipping towards the NW. Thus, the reservoir is located in on the footwall of the northern segment, and on the hanging wall of the southern segment. Figure 4 shows that most of the epicentres are located along the northern segment of Renzishi fault (2) in region C.

The Daping-Yanqian fault (3) is another steeply-dipping (60° to 90°) reverse fault. As it directly intersects the reservoir, it can be assumed that half of the reservoir is located on its hanging wall and half is situated on its foot wall, resulting in the effects from the oscillating reservoir load on the fault being small. It should be noted that the region C where earthquakes frequently occurred is on the footwall of Daping-Yanqian fault (3).

The Shijiao-Xingang-Baitian fault (4) is a vertical strike-slip fault. Based on the fault location theory, seismicity due to oscillating reservoir loads can occur in the fault region since the fault intersects the reservoir and the middle segment is directly beneath the reservoir. Earthquake focal mechanisms indicate that Shijiao-Xingang-Baitian fault (4) is the seismogenic fault that is responsible for the 19th March 1962 M_s 6.1 earthquake (Ding, 1989).

Based on the study of the above four major faults in the Xinfengjiang reservoir region, it can be seen that the fault location theory proposed by Roeloffs (1988) can effectively explain the spatial distributions of epicentres in the Xinfengjiang area. The effects on major faults in the reservoir area are summarised in Figure 5.

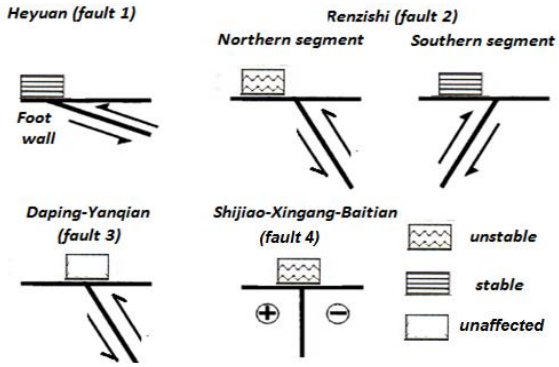

Figure 5: The effects of oscillating reservoir loads on major faults in the vicinity of Xinfengjiang reservoir (Based on Roeloffs, 1988)

3.2 Fault Orientation and Slip Tendency

The majority of the RIS cases are caused by the reactivation of existing discontinuities rather than the development of new faults (Morris et al., 1996). The possibility of reactivation for major faults in the Xinfengjiang area can be evaluated based on their orientations with respect to the regional stress field. The slip-tendency analysis is carried out using a MATLAB plug-in application (Neves et al., 2009) based on the Morris et al. (1996)'s definition of slip tendency(T_s): the ratio of resolved shear stress (τ) to resolved normal stress (σ_n) on a fault surface:

$$T_s = \frac{\tau}{\sigma_n} \quad (1)$$

The result of fault slip tendency analysis (Figure 6) indicates that the fault striking in the NNW direction Shijiao-Xingang-Baitian fault (4), has the highest slip tendency of 0.7. The three faults striking in a NE/NNE direction are less likely to slip.

3.3 Permeability Structure of Faults

Faults are considered as structurally anisotropic and lithologically heterogeneous. In terms of permeability, they can either assist or impede water flow depending on their permeability structures (Caine et al., 1996). Permeability structures of fault groups in the Xinfengjiang area are summarised in Table 2.

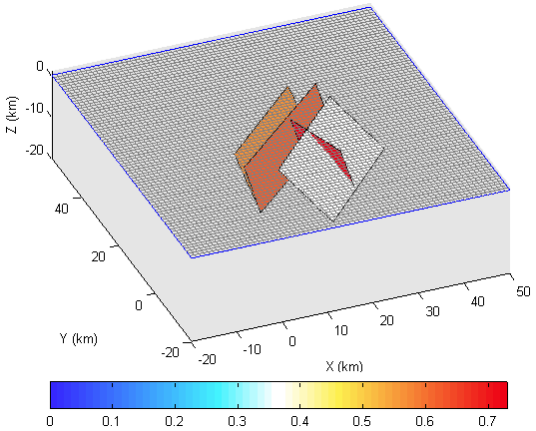

Figure 6: Slip-tendency analysis: Xinfengjiang reservoir region grid in 3D view with faults coloured by their individual slip-tendency value.

Fault Group	NNW (4)	NE/NNE (1), (2), (3)
Fault types	Strike-slip	Reverse
Fault core	partly filled with quartz veins	10-30m wide with siliceous rocks
Damage zone	Well developed	Poorly Developed
Fault rock	Granite	Granite
Activity	Movement in Pleistocene	No neotectonic movement
Permeability Structure	Distributed conduit	Localised barrier

Table 2: Characteristics of fault structures of the Xinfengjiang reservoir area, including permeability

The NE/NNE faults in the vicinity of Xinfengjiang reservoir are reverse faults with localised barrier type of permeability structures. In these localised barrier permeability structures, fault rocks are usually ductile in nature. The damage zone is not developed and the fault wall is poorly cemented. As there are no circulating paths for water to diffuse in this type of fault, RIS is unlikely to be triggered. The NNW faults are strike-slip faults where distributed conduit type of permeability structures are prone to form. The possibility of RIS is largest in this distributed conduit permeability structure as its fault core is widely spaced and poorly compacted with brittle fault rock. Also, the damage zone is well developed.

3.4 Fracture Permeability

Fracture permeability in the Xinfengjiang area is estimated to see if it lies within the seismogenic permeability range proposed by Talwani et al. (2007). Fractures that have their permeability within the seismogenic permeability range can allow pore water to diffuse as Darcian flow, thus making it easier to induce seismicity. However if the fracture permeability is lower than the seismogenic permeability, then the flow through the fracture is negligible, causing only a small pore pressure increases. If the fracture permeability is higher than the seismogenic permeability, then the flow rate is too large to act as a Darcian flow, and pore pressure diffusion is unlikely to occur. The fracture permeability can be estimated using the method of Talwani and Acree (1984):

$$k = c\mu[\eta\beta_f + (1-\eta)\beta_r] \quad (2)$$

where η is the porosity of the rocks, μ is the fluid viscosity, β_f and β_r are the compressibility of fluid and rock respectively. Hydraulic diffusivity c of the connecting fractures can be approximated by:

$$c = \mathrm{r}^2/4\Delta t \quad (3)$$

where Δt is the time lag between the reservoir impoundment and the beginning of seismicity. r is the distance from reservoir to the hypocentre of the earthquake.

The estimated hydraulic diffusivity values (1m/s to 5m²/s) correspond to a permeability value range of 5×10^{-15} m^2 to 2.5×10^{-14} m^2. This range of fracture permeability values are within the seismogenic permeability range. Therefore, RIS is likely to occur in the vicinity of Xinfengjiang reservoir.

Thus, analysis of slip tendency and permeability structure indicate that the NNW Shijiao-Xingang-Baitian fault (4) is the seismogenic structure, responsible for the majority of earthquakes in the Xinfengjiang reservoir area, including the M_s 6.1 main shock.

3.5 Reservoir Filling History

Before 1965 there was a good correlation between reservoir level and seismicity (Figure 7). The period of 1962 to 1964 is classified as a period of delayed response, when major earthquakes occur sometime after peak reservoir level is attained. (Qiu, 2012). However the M_s 5.1 and M_s 5.3 earthquakes occurred immediately after the exceedance of previous peak water level.

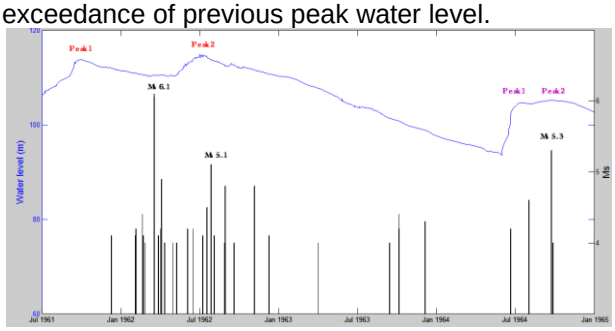

Figure 7: Water level fluctuation and earthquakes with $M_s \geqslant 4$ (Jul 1961-Jan 1965). Peak 1 represents the previous maximum water level, peak 2 represents the time when the previous maximum water level is exceeded.

One possible explanation could be the Kaiser effect, which describes the phenomenon that if a material is experiencing cyclic loading with increasing stress, there is an increase in micro seismicity (in the form of acoustic emission) if the highest stress level of the previous loading cycle (maximum water level) is exceeded (Lavarov, 2003).

This raises the question of why the M_s 6.1 main shock did not occur immediately after the first peak water level, but occurred when the water level was decreasing.

One possible explanation could be although the water level is decreasing, the pore pressure at the hypocentre of the M_s 6.1 earthquake is still increasing. This hypothesis is only true if pore pressure diffusion is the dominant mechanism, since both the vertical elastic stress increase and undrained pore pressure increase due to compression are short term effects. Thus it is vital to find out which is the dominant mechanism for inducing the M_s 6.1 main shock.

The Mohr-Coulomb failure model developed in Section 2.2 indicates that the increase in vertical stress has negligible effect on triggering seismicity since in strike-slip faulting regime, where Xinfengjiang reservoir is located, the vertical stress is neither the maximum nor the minimum principal stress. This implies that RIS is only triggered by either the instantaneous undrained pore pressure increase due to elastic compression or pore pressure diffusion. To evaluate their relative importance, the magnitudes of each are estimated below.

The maximum undrained pore pressure increase at the hypocentre of the main shock is estimated to be around 70kPa using the Skempton effect (Talwani & Acree, 1984):

$$\Delta P_u = B\bar{\sigma} \tag{4}$$

where B is the Skempton's coefficient and $\bar{\sigma}$ is the average change in stress. The diffused pore pressure is estimated based on Durá-Gómez and Talwani (2009)'s equation where

$$P_n = \delta p_1 \mathrm{erfc}\left(\frac{r}{(4cn\delta t)^{0.5}}\right) + \delta p_2 \mathrm{erfc}\left(\frac{r}{(4c(n-1)\delta t)^{0.5}}\right) + \cdots + \delta p_n \mathrm{erfc}\left(\frac{r}{(4c\delta t)^{0.5}}\right) \tag{5}$$

The diffusion time is divided into different intervals δt. The total pore pressure diffused to a point of r distance from the reservoir after n days (P_n) is equal to the sum of diffused pore pressure generated by water load changes in each time interval. For example, the reservoir water level change during the first time interval will contribute for n days to the total pore pressure diffused while the water level change during the second time interval will only contribute for n-1 days and so on.

If t and z are the time of an earthquake and the distance from reservoir to the hypocentre respectively, then this estimated diffused pore pressure value (P_n) can be interpreted as the threshold of the diffused pore pressure for that particular earthquake. Table 3 shows the range of threshold diffused pore pressure for 50 $M_s \geq 4$ earthquakes in the Xinfengjiang reservoir area during the period of 1961 to 2008.

	Threshold diffused pore pressure (Pa)		
Range	c=1m/s²	c=2.5m/s²	c=5m/s²
Maximum	604	652	680
Minimum	281	420	502

Table 3: Threshold diffused pore pressure values with varying hydraulic diffusivities (c).

The threshold pore pressures vary from 281kPa to 680 kPa, much larger than the undrained pore pressure increase, implying pore pressure diffusion should be the dominant mechanism in increasing pore pressure and reducing the effective stress. As the effect of undrained pore pressure increase due to elastic compression is instantaneous, by the time pore pressure front diffuses to the hypocentral location, this undrained effect may have already disappeared. Thus, the threshold of the diffused pore pressure can be interpreted as the threshold pore pressure for inducing seismic events.

However, the threshold pore pressure values only indicate the pore pressure required to trigger an earthquake at a particular location, such as the epicentre of the M_s 6.1 main shock, it does not effectively explain why this main shock occurred during a period of decreasing water level. To explain this phenomenon, a MATLAB model is built to model the pore pressure diffusion history at the hypocentre of the M_s 6.1 main shock (Figure 8).

Several important observations can be made from Figure 8. Firstly, the shape of pore pressure diffusion and water level fluctuations appear to be very similar, indicating a direct correlation. Secondly, the variations of the diffused pore pressure at hypocentral locations are dependent on the value of hydraulic diffusivity (c). When the hydraulic diffusivity is higher ($c=5m/s^2$), the diffused pore pressure will rise or diminish faster after experiencing a water level change, compared to low values of diffusivity. In addition, for the lower diffusivity case ($c=1m/s^2$), there is a delay between the reservoir impoundment and the onset of pore pressure increase. The initial increase in pore pressure for the lower diffusivity case is negligible. This delay of pore pressure could be due to the fact it takes longer for pore pressure front to arrive at the hypocentral locations for such low diffusivity values.

Figure 8(b) indicates that before the occurrence of M_s 6.1 main shock, although the water level was decreasing, the diffused pore pressure at the hypocentre was stilling increasing. This can be seen to confirm our hypothesis at the outset of this subsection. A similar pattern is observed for the M_s 4.1 earthquake on 20th Feb 1962 foreshock. The rate of pore pressure increase is higher during the foreshock period than during the main shock,

indicating that in the long term, if the water fluctuations are small compared to the initial filling stage, the diffused pore pressure at a particular location may slowly diminish through time.

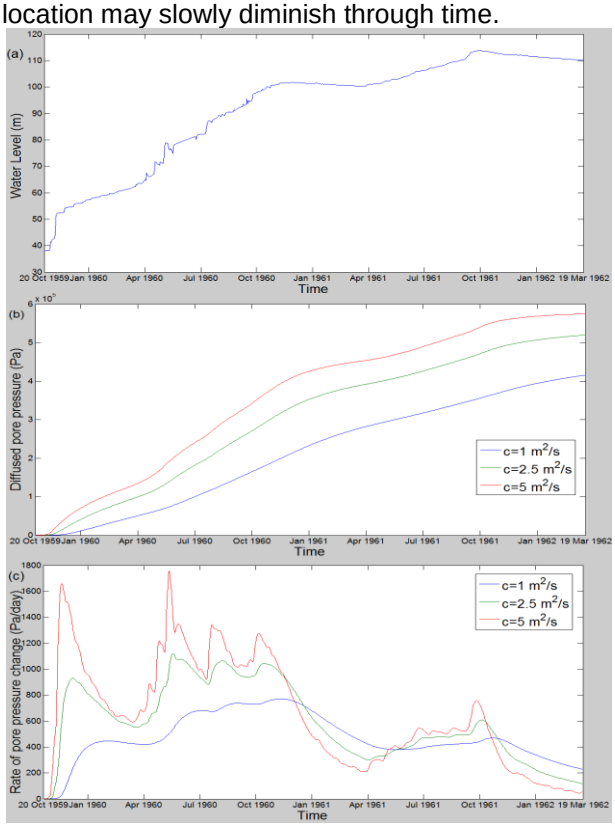

Figure 8: Water level fluctuation (a), pore pressure diffusion history (b) and rate of pore pressure change (c), at the hypocentre of 19th Mar 1962 M_s 6.1 main shock.

However for the aftershock event of M_s 4.3 on 6th December 1963, both the water level and the diffused pore pressure at the hypocentre were decreasing. This implies that failure of a fault does not always occur when the effective stress is the smallest. Future approaches to explain this phenomenon should focus on earthquake-induced hydrological changes and deviatory effects of pore pressure drop (Qiu, 2012).

4. CONCLUSION

In summary, in the case of Xinfengjiang reservoir, it appears that the evolution of the hydrogeological regime of the reservoir area plays the most important role in triggering seismicity. Concurrently, the stress regimes and the filling history can also be seen to contribute significantly in triggering seismicity. As the present study suggests, it should be emphasised that whether RIS will occur or not depends on a number of complex and interrelating factors. A combination of factors is required to trigger seismicity, of which no single factor has overwhelming control. The hydrogeological conditions themselves are in turn affected by induced earthquakes.

This study focuses on the case of Xinfengjiang reservoir, China. In order to further a more comprehensive understanding of the mechanisms, a series of case comparisons should be performed. Also, the modelling of pore pressure diffusion history is a promising approach as it allows investigation of RIS sensitivity in relation to the hydrological conditions at hypocentral depths. Further research could employ such approach to investigate the pore pressure diffusion history in relation to other RIS cases.

Reservoir induced earthquakes are possible but not an inevitable consequence of the impoundment of a reservoir. Because of the complexity and variety of factors, any strategy for the limitation of hazards due to reservoir impoundment should consider the overall complexity of the phenomenon. It is most important therefore to maintain focus on the interrelation of diverse concurrent factors rather than to isolate any single one of them. The data and research available strengthens the conclusion that, only when a combination of factors are present, seismicity can be triggered, and not the idea that any one single fact might play an overwhelming role in the process.

5. ACKNOWLEDGEMENTS

My deepest gratitude goes first and foremost to Dr. Clark Fenton, my supervisor for his constant encouragement, precious direction and insightful suggestion. I am particularly grateful for his patience and guidance throughout the project period. I also would like to express my gratitude to Jeong Min Han for his valuable advice.

6. REFERENCES

Caine, J. S., Evans, J. P. & Forster, C. B. (1996) Fault zone architecture and permeability structure. *[J]. Geology*, 24(11), 1025-1028

Cornet, F. & Yin, J. (1995) Analysis of induced seismicity for stress field determination and pore pressure mapping. *Pure Appl. Geophys*, 145, 677-700

Ding, Y. Z. 1989. Reservoir-induced Seismicity. Beijing, Seismological Press (in Chinese).

Durá-Gómez, I. & Talwani, P. (2009) Hydromechanics of the Koyna-Warna region, India. *Pure Appl. Geophy.* 167 (1-2), 183-213

Fyfe, W., Price, N. & Thompson, A. (1978) Fluids in earth's crust: Their significance in metamorphic, tectonic and chemical transport processes. Oxford, Elsevier

Lavarov, A. (2003) The Kaiser effect in rocks: principles and stress estimation technique. *Intl. J. Rock Mech & Mining Sciences,* 40, 151-171

Morris, A., Ferril, D. & Henderson, D. (1996) Slip-tndency analysis and fault reactivation. *Geology* 24, 275-278

Neves, M., Paiva, L. & Luis, J.Software for slip-tendency analysis in 3D: A plug-in for Coulomb. *Computers & Geosciences*, 35 (2009), 2345-2352.

Qiu, X. (2012) Reservoir-induced Seismicity. unpublished MEng dissertation, Imperial College, London, pp101-113.

Roeloffs, E. (1988) Fault stability changes induced beneath a reservoir with cyclic variations in water level. *J.Geophys.Res*, 93 (B3), 2107-2124.

Talwani, P. & Acree, S. (1984) Pore pressure diffusion and the mechanism of reservoir induced seismicity. *PAGEOPH* 122, 947-964

Talwani, P., Chen, L. & Gahalaut, K. (2007) Seismogenic permeability, ks. *J.Geophys Res*, 112 (B07309)